Protein Structure and Folding:

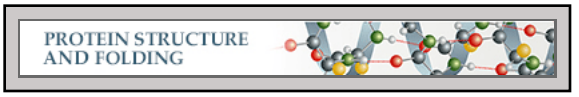

High Resolution Crystal Structures of Piscine Transthyretin Reveal Different Binding Modes for Triiodothyronine and Thyroxine

Therese Eneqvist, Erik Lundberg, Anders Karlsson, Shenghua Huang, Cecília R. A. Santos, Deborah M. Power and A. Elisabeth Sauer-Eriksson

J. Biol. Chem. 2004, 279:26411-26416.
doi: 10.1074/jbc.M313553200 originally published online April 13, 2004

THE JOURNAL OF BIOLOGICAL CHEMISTRY
Vol. 279, No. 25, Issue of June 18, pp. 26411–26416, 2004

Printed in U.S.A.

High Resolution Crystal Structures of Piscine Transthyretin Reveal Different Binding Modes for Triiodothyronine and Thyroxine*

Received for publication, December 11, 2003, and in revised form, March 16, 2004
Published, JBC Papers in Press, April 13, 2004, DOI 10.1074/jbc.M313553200

Therese Eneqvist‡§, Erik Lundberg‡, Anders Karlsson‡, Shenghua Huang‡, Cecília R. A. Santos¶, Deborah M. Power¶, and A. Elisabeth Sauer-Eriksson‡‖

From the ‡Umeå Centre for Molecular Pathogenesis, Umeå University, SE-901 87 Umeå, Sweden and the ¶Centro de Ciencias de MAR, Universidade do Algarve, Campus de Gambelas, 8005–139 Faro, Portugal

Transthyretin (TTR) is an extracellular transport protein involved in the distribution of thyroid hormones and vitamin A. So far, TTR has only been found in vertebrates, of which piscine TTR displays the lowest sequence identity with human TTR (47%). Human and piscine TTR bind both thyroid hormones 3,5,3′-triiodo-L-thyronine (T_3) and 3,5,3′,5′-tetraiodo-L-thyronine (thyroxine, T_4). Human TTR has higher affinity for T_4 than T_3, whereas the reverse holds for piscine TTR. X-ray structures of *Sparus aurata* (sea bream) TTR have been determined as the apo-protein at 1.75 Å resolution and bound to ligands T_3 and T_4, both at 1.9 Å resolution. The apo structure is similar to human TTR with structural changes only at β-strand D. This strand forms an extended loop conformation similar to the one in chicken TTR. The piscine TTR·T_4 complex shows the T_4-binding site to be similar but not identical to human TTR, whereas the TTR·T_3 complex shows the I3′ halogen situated at the site normally occupied by the hydroxyl group of T_4. The significantly wider entrance of the hormone-binding channel in sea bream TTR, in combination with its narrower cavity, provides a structural explanation for the different binding affinities of human and piscine TTR to T_3 and T_4.

Transthyretin (TTR)[1] is one of three proteins in the extracellular fluids of vertebrates responsible for the distribution of the two thyroid hormones 3,5,3′-triiodo-L-thyronine (T_3) and 3,5,3′,5′-tetraiodo-L-thyronine (thyroxine, T_4) (1). TTR also transports vitamin A by forming a complex with retinol-binding protein (for reviews, see Refs. 2 and 3). Although members of a related protein family were identified in lower species (4), TTR homologues have only been found in vertebrates and share high sequence identity. Of these orders, piscine TTR has the lowest sequence identity compared with human TTR. The first complete cDNA sequence of a piscine transthyretin homologue was isolated from sea bream (*Sparus aurata*) and has 47% sequence identity with human TTR (5–7). Interestingly, piscine TTR displays a higher affinity for T_3 than T_4 (7, 8), as do the amphibian and avian TTRs. This is in contrast to the marsupial and mammalian proteins, which have higher affinity for T_4 (9, 10). In birds, marsupials, and mammals, TTR is expressed both in the liver and choroid plexus of the brain, whereas in reptiles it is expressed only in the choroid plexus. In fish or amphibians the main production is in the liver (2, 3, 11). This suggests that the binding affinities of TTR changed during evolution. In mammalian TTR, transport of T_4 is preferred across the blood-brain barrier, where T_4 is converted to the biologically more active T_3 hormone (12). This evolution may correlate with the evolution of deiodinases, which generate T_3 from T_4 in a tissue-specific action (12, 13).

The three-dimensional structure of transthyretin is a homotetramer with a central hydrophobic channel in which the two hormone-binding sites are situated (14–17). The two retinol-binding protein-binding sites have also been structurally characterized and are situated on the surface of the molecule (18, 19). Previously determined structures of chicken, rat, and human TTR are very similar, with the exception of the α-helical region, which is somewhat different in the avian structure compared with the mammalian proteins (20, 21).

Single point mutations in human transthyretin give rise to familial amyloidotic polyneuropathy (FAP), a hereditary form of amyloidosis associated with fibrillar TTR deposits in the peripheral nerves, kidney, spleen, heart, and eye (22–24). More than 70 different amino acid substitutions related to FAP have been identified so far (25), two of which are present in the sea bream TTR sequence, namely V30L and I84S (26). Structural changes within the TTR molecule underlie the formation of TTR amyloid fibrils (27, 28). To elucidate the mechanism behind TTR amyloidosis, structural analyses of TTR from other organisms can provide valuable information. This study describes three crystal structures: apo sea bream TTR at 1.75 Å resolution; in complex with T_3 at 1.9 Å; and in complex with T_4, also at 1.9 Å. The structures are compared with the human, rat, and chicken homologues, and molecular details behind thyroid-hormone binding are discussed.

MATERIALS AND METHODS

Cloning of Sea Bream TTR—A construct corresponding to the mature sea bream TTR, predicted by SignalP v1.1 (29), was amplified from the full-length cDNA located in a PA20H vector (7) using the forward primer 5′-TTT TTC ATG ACC CCC ACC CCC ACG-3′ (Interactiva Virtual Laboratory). This primer introduces the N-terminal methionine and a BspH1 cleavage site, which changes the first Ala-19 codon GCC to ACC that encodes Thr. The reverse primer 5′-TTT CGA GCT CAC TCG TGT ACG CTG GAG-3′ (Interactiva Virtual Laboratory) introduces a flanking SacI cleavage site following the C-terminal stop codon.

* This study was supported by the Swedish Science Council (K2001-03X-13001-03A) and the patients' association FAMY/AMYL (to E. S.-E). The costs of publication of this article were defrayed in part by the payment of page charges. This article must therefore be hereby marked "*advertisement*" in accordance with 18 U.S.C. Section 1734 solely to indicate this fact.

The atomic coordinates and structure factors (codes 1SN2 and RCSB021842, 1SN0 and RCSB021841, and 1SN5 and RCSB021843) have been deposited in the Protein Data Bank, Research Collaboratory for Structural Bioinformatics, Rutgers University, New Brunswick, NJ (http://www.rcsb.org/).

§ Present address: Dept. of Biochemistry and Biophysics, Stockholm University, SE-106 91 Stockholm, Sweden.

‖ To whom correspondence should be addressed. Tel: 46-90-7856782; Fax: 46-90-778007; E-mail: liz@ucmp.umu.se.

[1] The abbreviations used are: TTR, transthyretin; T_3, 3,5,3′-triiodo-L-thyronine; T_4, 3,5,3′,5′-tetraiodo-L-thyronine (thyroxine); MME, monomethyl ether; HBP, halogen-binding pocket.

TABLE I

Data collection, refinement, and structural statistics for the sea bream TTR structures

$R_{merge} = \sum_h \sum_i | I_{ih} - \langle I_h \rangle | / \sum_h \sum_i \langle I_h \rangle$, where $\langle I_h \rangle$ is the mean intensity of the i observations of reflection h. R-factor $= \sum \| F_{obs}| - |F_{calc}\| / \sum |F_{obs}|$, where $|F_{obs}|$ and $|F_{calc}|$ are the observed and calculated structure factor amplitudes, respectively. Summation includes all reflections used in the refinement. R_{free} is evaluated for a randomly chosen subset comprising 10% of the diffraction data not included in the refinement. R.m.s.d. is the root mean squared deviation from ideal values.

	TTR (apo)	TTR·T_3	TTR·T_4
Data collection			
Space group	$P4_1$	$P4_1$	$P4_1$
Cell dimensions (Å)	$a = b = 58.50$	$a = b = 58.28$	$a = b = 58.46$
	$c = 140.71$	$c = 138.90$	$c = 140.12$
Resolution	50–1.75	20–1.90	20–1.90
(Highest resolution shell) (Å)	(1.81–1.75)	(1.97–1.90)	(1.97–1.90)
Number of observations	928494	305833	395502
Unique reflections	46104 (4416)	36032 (3581)	35498 (3244)
Completeness (%)	97.1 (92.2)	98.8 (96.6)	96.0 (89.7)
R_{merge} (%)	4.7 (45.1)	5.4 (43.4)	4.7 (44.6)
Refinement			
Resolution range used in refinement (Å)	20–1.75	20–1.9	20–1.9
Reflections in working set	39742	31100	30446
Reflections in test set	4439	3405	3336
R-factor working set (%)	17.5	17.3	17.9
R_{free} test set (%)	21.0	21.1	21.6
Mean temperature factor (Å^2)	21.6	14.4	14.6
R.m.s.d. bond lengths (Å)	0.008	0.010	0.009
R.m.s.d. bond angles (°)	1.30	1.46	1.40
Torsion angles period 1 (°)	3.96	4.01	4.04
Torsion angles period 3 (°)	18.39	18.30	18.30

After digestion with BspH1 and SacI (New England Biolabs/Amersham Biosciences), the fragment was introduced into a pET24d vector (kindly provided by Gunter Stier, EMBL-Heidelberg, Germany) cleaved with SacI and NcoI using the T4 DNA ligase Ready-To-Go kit (Amersham Biosciences). The ligated vector was used to transform (30) *Escherichia coli* DH5α and plated on Luria Bertani agar plates containing 30 μg ml^{-1} kanamycin, after which all transformants were collected for plasmid preparation using Wizard Plus SV minipreps (Promega). The plasmids were digested with BamH1 (New England Biolabs), whose cleavage site is situated within the region of the pET24d cloning cassette supposedly replaced by the TTR gene, and used for a second transformation (30) of DH5α plated on 30 μg ml^{-1} kanamycin Luria Bertani agar plates. The cloned sea bream TTR gene was sequenced using the DYEnamic ET terminator kit (Amersham Biosciences) and an ABI 377 sequencer.

Protein Expression and Purification—Competent *E. coli* BL21 cells were transformed (30) with the pET24d vector containing the sea bream TTR construct and plated onto Luria Bertani agar plates containing 30 μg ml^{-1} kanamycin. One colony was selected and grown in Luria Bertani with 30 μg ml^{-1} kanamycin at 30 °C to A_{600} nm = 0.9, induced with 0.2 mM isopropylthiogalactoside overnight, harvested by centrifugation, and stored at −20 °C. Frozen cells were thawed and lysed in 10 ml of water that included ~1 mg of lysozyme and $MgCl_2$ for 10 min. DNase I was added, followed by incubation for another 10 min and centrifugation at 25,000 × g for 20 min. The supernatant was loaded onto a 10% preparative native PAGE (Model 491 Prep Cell; Bio-Rad) equilibrated with 0.025 M Tris, pH 8.5, and 1.9 M glycine. Protein fractions were analyzed by 20% SDS-PAGE; those containing pure sea bream TTR were pooled, dialysed against 50 mM Tris, pH 7.5, concentrated to 5 mg ml^{-1} (Centriprep; Amicon) and stored at −20 °C.

Crystallization and Data Collection—All crystals were grown using the hanging-drop vapor-diffusion method (31). Drops with 8 μl of a 5 mg ml^{-1} solution of sea bream TTR in 50 mM Tris, pH 7.5, were mixed with 2 μl of well solution containing 40–44% polyethylene glycol 550 monomethyl ether (MME), 100 mM sodium citrate, pH 5.0, 100 mM ammonium sulfate, and 26 mM nickel sulfate or cobalt chloride and equilibrated at room temperature. Crystals 0.3 × 0.3 × 0.4 mm^3 appeared in 7 days and diffracted to 1.75 Å resolution. The crystals belonged to the tetragonal space group $P4_1$ with one tetramer in the asymmetric unit. Crystals of the two TTR·hormone complexes diffracted to 1.9 Å resolution. Both complexes were crystallized in a similar fashion, *i.e.* the apo protein was incubated for 24 h at 4 °C with a saturated solution of T_3 or T_4 in 50 mM Tris, pH 7.5, prior to the crystallization trials. All data sets were collected at 100 K from single crystals mounted in nylon loops (32), using synchrotron radiation at beam line X11, European Molecular Biology Laboratory outstation, German Synchrotron Research Centre, Hamburg, Germany. The data were processed and scaled with the programs DENZO and SCALEPACK (33), after which the intensities were converted to structure factors using the programs TRUNCATE and CAD from the CCP4 package (34). Data collection statistics are included in Table I.

Molecular Replacement and Structure Refinement—The structure of the apo protein was solved by molecular replacement using the program package CNS (35). A poly(alanine) model of the human transthyretin tetramer was used as starting model (Protein Data Bank code 1F41, Ref. 16) with the BC loops (residues 36–40), CD loops (residues 50–52), α-helices (residues 80–86), and FG loops (residues 98–104) removed. The progress of refinement was followed by monitoring the R_{free} value from the start, with 10% of the reflections included in the test set (36). After rigid body refinement, nearly all side chains could be manually built into the first $2F_o - F_c$ map using the graphics software O (37). The structure was refined by subsequent positional and temperature factor refinement using CNS (35), REFMAC (38), and manual model building. The hormone complexes were refined with REFMAC (38) by means of difference Fourier techniques using the structure of the piscine apo protein. The coordinates for T_3 and T_4 were derived from the Heterocompound Information Centre (39). The refined models comprise good stereochemistry according to PROCHECK (40). Refinement statistics are presented in Table I. Pictures were generated using the programs MOLRAY (41), MOLSCRIPT (42), and RASTER3D (43).

Atomic coordinates and structure factors have been deposited in the Research Collaboratory for Structural Bioinformatics (RCSB) with the following accession codes: 1SN2 and RCSB021842 (apo fish TTR), 1SN0 and RCSB021841 (T_4 complex), and 1SN5 and RCSB021843 (T_3 complex).

RESULTS AND DISCUSSION

The Structure of Piscine Transthyretin—The structure of sea bream TTR was solved using molecular replacement methods with a truncated poly(alanine) model of human TTR (PDB accession code 1F41, Ref. 16) as a search model. The quality of the initial electron density map was excellent and allowed most side chains of the fish TTR structure to be modeled. The four monomers (A, B, C, and D) comprising the tetramer in the asymmetric unit were refined independently of each other from the start. The final model includes residues A10-A127, B10-B125, C11-C125, D10-D123, 361 water molecules, and one sulfate ion (Fig. 1). In some cases, additional electron density was observed at the N- and C-terminal ends, but the quality did not allow additional residues to be exclusively positioned. The side chains of residues A-Gln-63, C-Glu-61, C-Gln-62, C-His-102, C-Ser-124, D-Gln-62, and D-Gly-101 displayed weak electron density. Seven residues were refined in two well defined conformations: A-Ser-84, A-Asp-96, B-Ser-84, B-Thr-119, C-Asp-96, C-Thr-119, and D-Thr-119. The 361 water molecules were positioned within

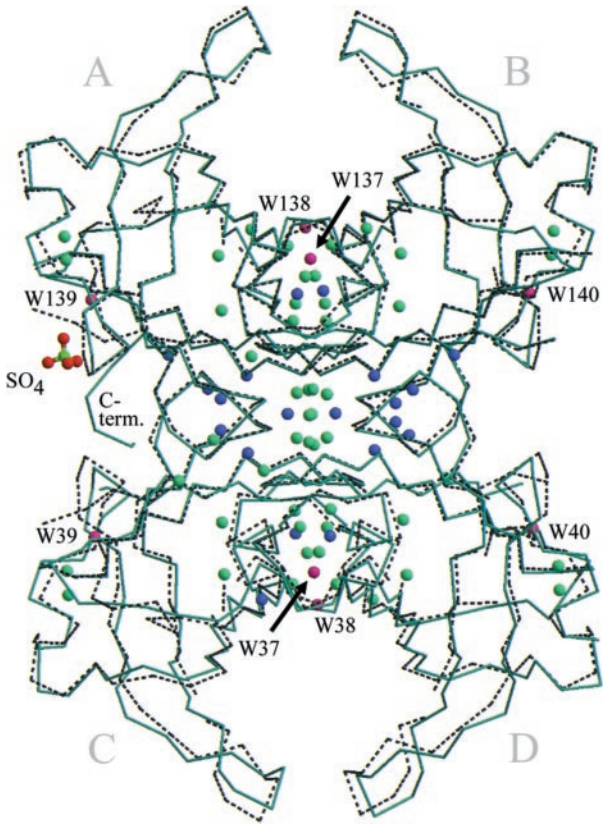

FIG. 1. **Cα trace of sea bream TTR (*cyan*) superimposed over the human protein (*dashed black lines*; Protein Data Bank code 1F41).** Water molecules unique for sea bream TTR are *pink*, those present in human TTR but absent in the fish structure are *blue*, and waters found in both structures are *green*. The sulfate group present in sea bream TTR is drawn as *ball-and-sticks*.

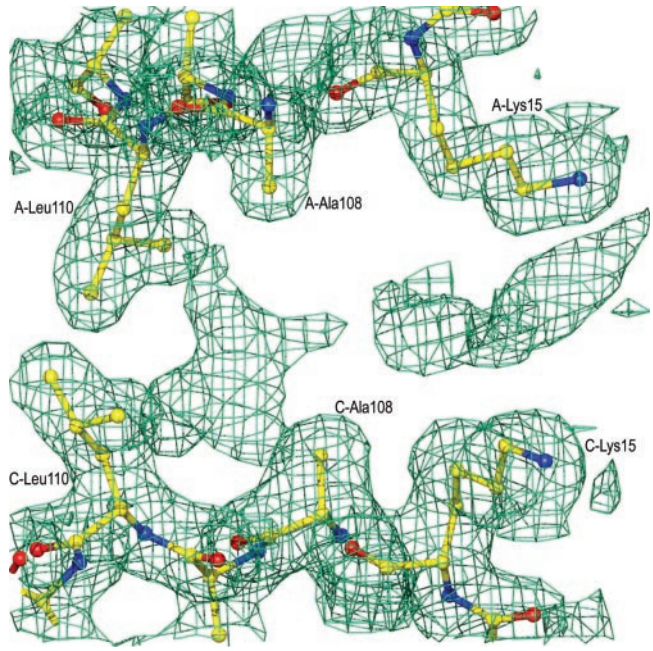

FIG. 2. **The 2 $F_o - F_c$ electron density map at the thyroid hormone-binding channel in sea bream apo TTR.** Contours are drawn at a level of 0.6σ, where σ is the root mean square density throughout the unit cell. The sea bream complex structures are drawn with carbons in *yellow*, nitrogens in *blue*, oxygens in *red*, and sulfurs in *green*.

proper hydrogen-bonding distances (less than 3.4 Å) from the protein with refined temperature factors less than 60 Å^2.

The four monomers in sea bream TTR are very similar. Root mean square deviations comparing the main chain Cα atoms of residues 12–123 among all monomers varies from 0.27 Å (comparing monomers A and B) to 0.51 Å (comparing monomers A and C). The sulfate ion bridges the main chain carbonyl oxygen of His-102 in the FG loop of monomer A and the Oγ atom of Ser-123 to the main chain nitrogen atom of Ser-124 at the C-terminal end of monomer A. This sulfate ion is also part of the crystal-packing interface forming a salt link to the side chain of Arg-103 in a symmetry-related copy of monomer B (B′). All sulfate atoms are well defined with B-factors of 34–36 Å^2 and restrict the mobility at the C-terminal end of monomer A, which could be modeled to the last residue, A-Glu-127.

The N terminus of piscine, avian, and reptilian TTR has three additional hydrophilic amino acids, DKH, compared with the eutherian proteins. A chimeric molecule generated from crocodile TTR, in which the N-terminal end was replaced by that from frog, was shown to differ in both the specificity and affinity of T_4 and T_3 binding. Therefore, it appears that the amino-terminal regions of TTR could influence its thyroid binding properties (13). Interestingly, in the sea bream structure, electron density runs through the center of the hormone-binding channel visible at lower contour levels of the electron density maps (Fig. 2). We could not identify the source of this density, but water molecules seem unlikely because the density does not connect to potential hydrogen-bonding partners on the protein. Two possibilities are that the electron density corresponds to residues at the N-terminal end of the protein or to polyethylene glycol molecules present in the crystallization medium.

While this work was in revision, a structure of sea bream TTR in a different crystal form was independently reported by Folli *et al.* (44). We find their structure virtually identical to ours with the exception of the positions of the FG loops. There have been controversies about the correct amino acid at position 103 (5, 7). By sequencing the clone, we would like to correct the original data published in Ref. 7 and confirm that the correct amino acid at position 103 should be an arginine. It should, however, be noted that the structure deposited by Folli *et al*. is reported to have a glycine at this position.

Comparison of Piscine TTR with Other Species—Crystal structures of TTR are available from three other species; human (16), chicken (20), and rat (21). Overall, the structure of sea bream TTR is very similar to those of rat and human with root mean square deviations of 0.62 and 0.71 Å, respectively, when superimposed on residues 12–98 and 104–123. Chicken TTR deviates significantly from fish, human, and rat in the conformation of the α-helix and succeeding EF loop (residues 75–88), and its root mean square deviation to sea bream TTR is 1.3 Å. These differences are most likely caused by a sulfate ion located in the α-helix region of the chicken structure, a different position compared with the sulfate found in sea bream TTR, that binds to the FG-loop (residues His-102 and Arg-103) and C-terminal (residues Ser-123 and Ser-124).

Water molecules W1-W36 play a significant role in stabilizing the monomeric (W1-W12), dimeric (W13-W20), and tetrameric (W21-W36) forms of the human protein (16). These water molecules are not strictly conserved in sea bream TTR, but all the corresponding molecules were numbered equivalent to human TTR (W1-W36 in monomers A and B and V1-V36 in monomers C and D) (Fig. 1). One novel water molecule is situated at the edge-strand region of each monomer, which is the only area with significant structural differences between human and piscine TTR. When comparing the two structures, the dissimilarity is already visible at the end of β-strand B, even more so in β-strand C, and most apparent in what corre-

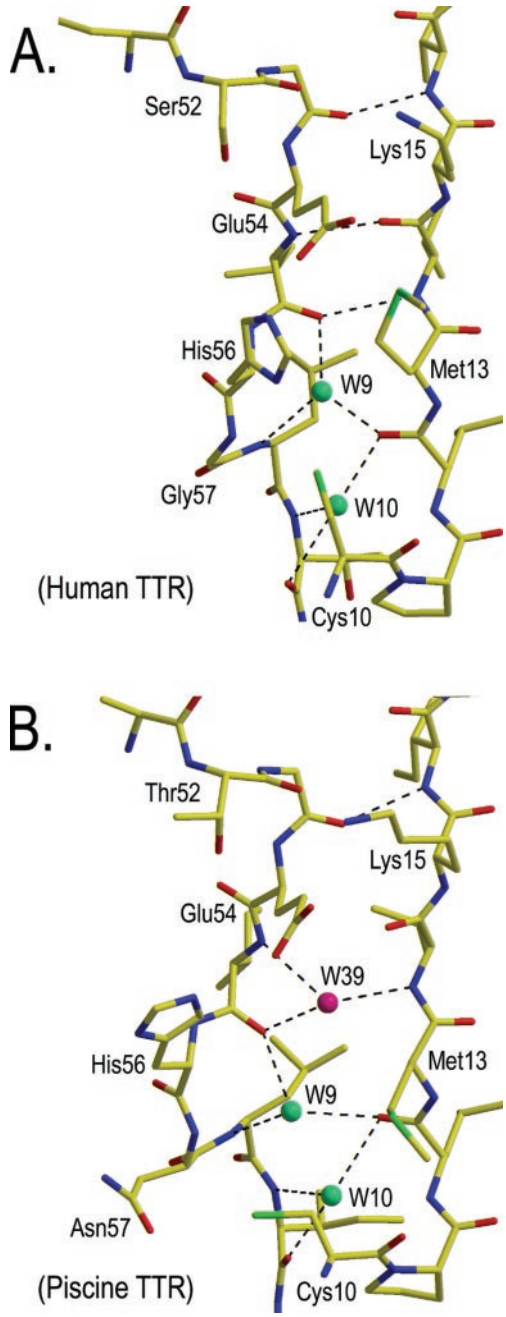

FIG. 3. **The conformation of β-strand D in monomer A.** *A*, human TTR. *B*, sea bream TTR. β-strand D, defined by three hydrogen bonds from residues Gly-53 and Leu-55 to residues Val-16 and -14 situated on β-strand A, are indicated as *black dashed lines* in the human structure. The novel water molecule W39 in sea bream is *pink*; waters W9 and W10 present in both structures are *green*.

sponds to β-strand D in human TTR. Sea bream TTR lacks a proper β-strand D and instead forms an extended loop region stabilized by a novel water molecule W39 (W40, W139, and W140 in the B, C, and D monomers, respectively). This water molecule bridges the D loop to β-strand A, forming hydrogen bonds to the main chain nitrogen and oxygen atoms of Ile-55 and the main chain nitrogen atom of Val-14 (Fig. 3, *A* and *B*). The piscine edge-strand conformation is reminiscent of chicken TTR, which also lacks β-strand D, whereas this area in the rat homologue is more similar to the human protein.

An analysis of human mutations associated with familial amyloidotic polyneuropathy compared with a multiple sequence alignment of the TTR sequences from 20 different species shows that only six familial amyloidotic polyneuropathy mutations occur as natural amino acids in other species (4). Leu-68 is found in eight species, Thr-45 in African clawed frog, Asp-42 and Ser-45 in bullfrog, and Leu-30 and Ser-84 in fish. The positions of both Leu-30 and Ser-84 are well defined in the electron density of sea bream TTR, but their structural significance is difficult to interpret because they are situated in regions with additional side chain substitutions compared with the human protein.

Hormone Binding to Sea Bream TTR—We have previously shown that the binding properties of T_3 and T_4 for purified recombinant sea bream TTR are similar to those for the endogenous serum protein in sea bream (4). The x-ray crystal structures of human TTR in complex with T_4 provide the first detailed description of a thyroid hormone binding to TTR (17, 45). These studies show that the two TTR hormone-binding sites, situated between monomers A, C and B, D, respectively, can be divided in three sections: an inner and outer cavity comprising three symmetry-related pairs of halogen-binding pockets, HBP1 (HBP1′), HBP2 (HBP2′), and HBP3 (HBP3′). The 2-fold symmetry axis of the TTR homotetramer runs in the direction of the hormone-binding channel and coincides with the 2-fold crystallographic symmetry axis in crystals with the $P2_12_12$ space group. However, most TTR ligands lack 2-fold symmetry, and subsequently the x-ray structures of human TTR complexes in the $P2_12_12$ space group have to be refined with the ligand positioned in two symmetry-related conformations with 50% occupancy. This complicates the electron density map interpretation and reduces the accuracy of the model. Recently, aligned thyroxine molecules were presented from structural studies of human and rat TTR crystals with tetramers rather than dimers in the asymmetric unit (46, 47). Interestingly, these structures show that ligand binding imposes subtle structural differences in the AC dimer compared with the BD dimer that is selected for in the crystal packing of the TTR tetramers. A multitude of structural data about TTR·ligand complexes is available (17, 45, 47–53). Combined, these studies show a complicated picture of TTR-ligand interactions where the same ligand can have more than one binding site in the hormone-binding channel.

T_4 comprises four iodines: I3 and I5 at the tyrosyl ring and I3′ and I5′ at the phenolic ring. In the human TTR·T_4 complex, the I3 and I5 iodines are situated at the outer HBP1 site, whereas I3′ and I5′ are situated at the innermost HBP2 and HBP3 sites (17, 45). The polar amino group interacts with the charged residues Lys-15 and Glu-54 at the entrance of the channel. In the structure of T_4 in complex with rat TTR, T_4 occupies two positions in the AC and BD-binding sites of the tetramer. One position is similar to T_4 in the human protein where the phenolic iodines occupy the HBP2/HBP3′ pocket; in the second position the phenolic iodines occupy the HBP3/HBP3′ pocket (47). The structure of human TTR in complex with T_3 is not known. We have made several attempts to obtain this structure but so far without success. We have collected high resolution diffraction data of both crystals soaked in T_3 and of co-crystals obtained at high concentration of T_3. In both cases, the determined protein structures represented the apo form of the protein. We did not detect any binding of T_3 to human recombinant TTR in the dot-blot analysis, which shows strong binding of T_3 to sea bream TTR (4). This suggests that binding of T_3 to human recombinant TTR is weaker than to the serum TTR protein.

The sea bream TTR complexes with T_3 and T_4 were each studied at 1.90 Å resolution. Generally, hormone binding did not induce any major structural changes and strand D maintained its extended loop conformation. The position of the three and four iodines in T_3 and T_4, respectively, could be clearly identified from omit maps (Fig. 4). However, the thyronine rings and alanyl moiety are less well defined in both complex structures. As in the

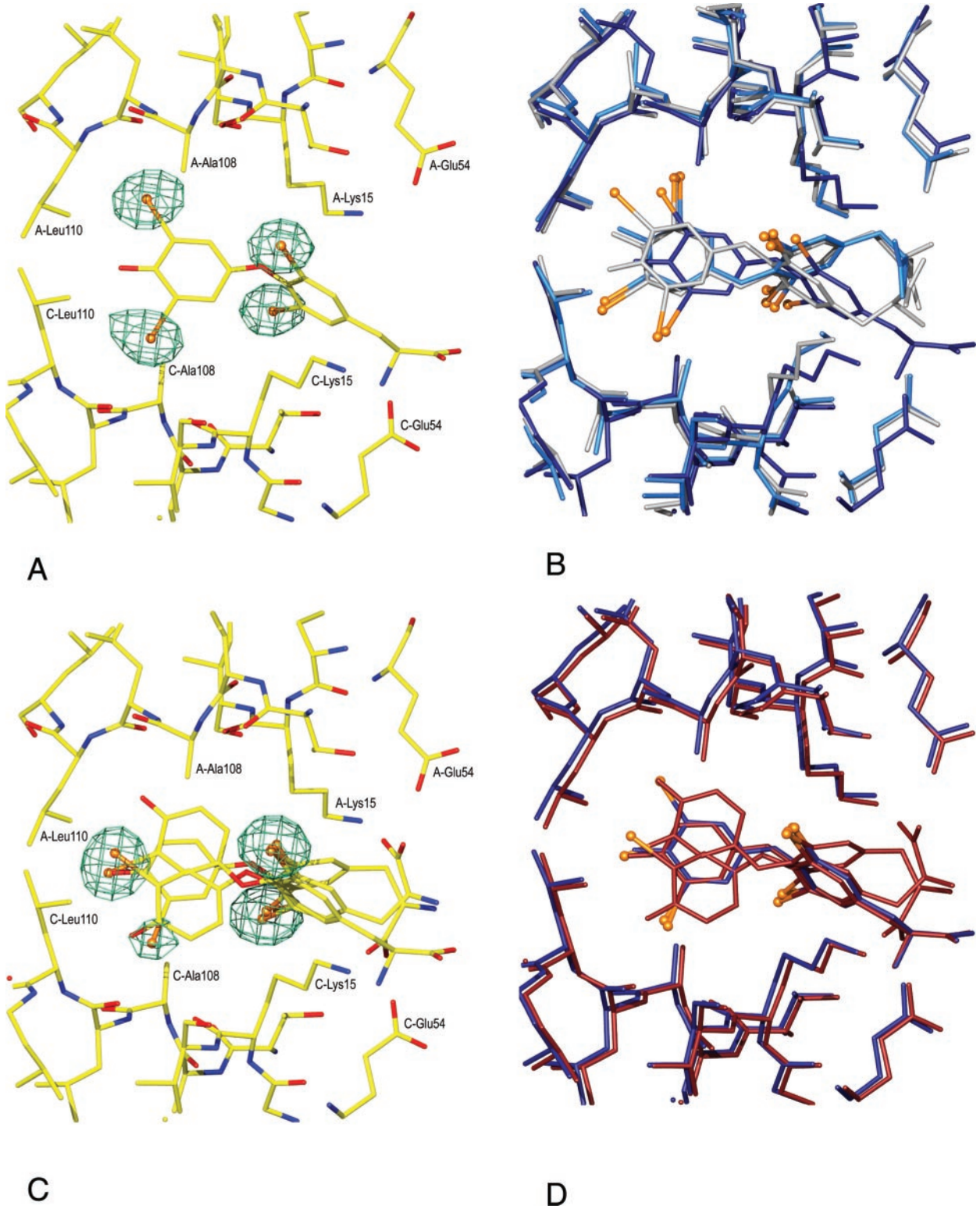

FIG. 4. T_4 and T_3 binding in monomer A of sea bream TTR (*A*) of the sea bream TTR·T_4 complex. *B*, T_4 binding to human TTR (*light gray*), rat TTR (*blue*), and sea bream TTR (*dark blue*). All structures are superimposed on residues A12-A98 and A104-A123. The T_4 molecule does not reach as deep into the hydrophobic channel of sea bream TTR as it does in human and rat TTR; thus, none of the four iodines binds to the HBP3. *C*, the sea bream TTR·T_3 complex. Three strong electron density features correspond to two equivalent positions of the T_3 ligand. The fourth and weaker electron density feature shows that a smaller fraction of the T_3 molecules is position equivalent to the T_4 molecule. This density is, however, not present in monomer B of sea bream TTR. *D*, comparison of T_4 (*dark blue*) and T_3 (*red*) binding to sea bream TTR. The sea bream complex structures in *panels A* and *C* are colored as in Fig. 2. Omit $F_o - F_c$ maps are contoured at 6σ over the hormone-binding site.

previously described human and rat TTR tetramers, the electron density maps display one unique binding mode of the T_4 hormone, suggesting that sea bream TTR tetramers are aligned within the crystals. T_4 binds similarly to sea bream TTR compared with human and rat TTR. However, the hormone molecule does not reach as deeply into the binding pocket and is situated ~1 Å closer to the entrance (Fig. 4*B*). This binding positioned the I3′ and I5′ atoms symmetrically at the halogen-binding pockets

HBP2 and HBP2′. Furthermore, the HBP3 and HBP3′ sites do not bind iodine in the piscine TTR·T_4 complex.

In the TTR·T_3 complex, four strong electron density features were observed in the AC-binding site, one of which is situated at the position of the hydroxyl group, O4′, in T_4. This site is now occupied to a large extent by the third iodine, I3′, in T_3 (Fig. 4*C*). In this novel T_3 conformation, the O4′ group is instead close to the main chain atoms of Leu-109 and -110 (distances are 3.0–3.2 Å). This position cannot be adopted by T_4 because it leaves no room for the additional I5′ atom (Fig. 4*D*). The electron density also shows that a small fraction (~20%) of T_3 is positioned identically to T_4. At the BD-binding site, electron density features for only three T_3 iodines were found. Thus the T_4-binding position is not occupied by T_3 in the BD-binding site. As in the piscine TTR·T_4 complex, there was no iodine in the HBP3-binding site in the TTR·T_3 complex. Further structural studies are needed to elucidate whether HBP3 of piscine TTR comprises a halogen-binding site or not.

Superimposing the sea bream TTR·T_3 structure with all available human TTR complex structures shows that the novel binding of T_3 to piscine TTR has a small resemblance to the binding of pentabromphenol and 2,4,6-tribromphenol to human TTR (53). Both bromphenols bind in the so-called "reversed" mode with their hydroxyl group directed toward the opening of the channel. One halogen of each ligand occupies the same position as the hydroxyl group in the human TTR·T_4 complex and the phenolic iodine I3′ in the sea bream TTR·T_3 complex.

With the exception of the number of water molecules within the apo proteins, the hormone-binding channels of sea bream and human TTR appear very similar. The only amino acid difference within the channel is the conservative substitution of Thr-117 in sea bream to Ser in human TTR, situated 4 Å away from the hormone molecule. However, the shape of the hormone-binding channel of sea bream and human TTR is different, which explains the discrepancies in T_3- and T_4 binding affinities of the two species. The areas of the cavity enclosing the inner phenolic and the outer tyrosyl rings of the hormone are clearly narrower in fish TTR. This is evident upon comparing the distance between two symmetry-related residues at position 108, which is 11.2 Å in sea bream TTR and 12.0Å in human TTR, and between the Cα atoms of two symmetry-related Lys-15 residues, 12.5–12.6 Å in fish TTR compared with 13.5–13.8 Å in human TTR. In addition, the sea bream TTR hormone-binding channel is wider at its entrance, right at the binding site for the alanyl group of the hormone. At the entrance, the distance between two Cα atoms of Glu-54 is 18.9–19.0 Å in sea bream TTR compared with 17.5–17.6 Å in the human protein. These dissimilarities are due in part to a number of amino acid substitutions in the hydrophobic core of fish TTR compared with the human protein, including Ile-16 for Val, Leu-30 for Val, Ile-44 for Phe, Ile-55 for Leu, Ile-59 for Thr, Phe-73 for Ile, Leu-109 for Ala. Furthermore, different side chain rotamers of Val-14 and Leu-58 affect the position of the otherwise conserved residues involved in hormone binding. The significantly wider entrance of the hormone-binding channel in combination with its narrower inner and outer cavity provides a structural explanation for the different binding affinities of T_3 and T_4 to avian and piscine TTR compared with human TTR. The inner phenolic ring of the T_3 molecule has only one iodine and is therefore smaller than the phenolic ring of T_4 and in its novel position in the outer tyrosyl ring is parallel to the Lys-15 side chains in a conformation optimal for the restricted channel of sea bream TTR. Avian TTR, which also has higher affinity for T_3 than T_4 (10), displays a similar overall shape as sea bream TTR.

Acknowledgements—We thank Anders Olofsson, Uwe H. Sauer, Andreas Hörnberg, and Terese Bergfors for valuable discussions and critical reading of the manuscript.

REFERENCES

1. Bartalena, L., and Robbins, J. (1993) *Clin. Lab. Med.* **13,** 583–598
2. Schreiber, G., and Richardson, S. J. (1997) *Comp. Biochem. Physiol. B Biochem. Mol. Biol.* **116,** 137–160
3. Power, D. M., Elias, N. P., Richardson, S. J., Mendes, J., Soares, C. M., and Santos, C. R. (2000) *Gen. Comp. Endocrinol.* **119,** 241–255
4. Eneqvist, T., Lundberg, E., Nilsson, L., Abagyan, R., and Sauer-Eriksson, A. E. (2003) *Eur. J. Biochem.* **270,** 518–532
5. Fünkenstein, B., Perrot, V., and Brown, C. L. (1999) *Mol. Cell. Endocrinol.* **157,** 67–73
6. Santos, C. R. A., and Power, D. M. (1996) *Ann. Endocrinol.* **57,** 58
7. Santos, C. R., and Power, D. M. (1999) *Endocrinology* **140,** 2430–2433
8. Yamauchi, K., Nakajima, J., Hayashi, H., and Hara, A. (1999) *Eur. J. Biochem.* **265,** 944–949
9. Yamauchi, K., Kasahara, T., Hayashi, H., and Horiuchi, R. (1993) *Endocrinology* **132,** 2254–2261
10. Chang, L., Munro, S. L., Richardson, S. J., and Schreiber, G. (1999) *Eur. J. Biochem.* **259,** 534–542
11. Santos, C. R., Anjos, L., and Power, D. M. (2002) *Clin. Chem. Lab. Med.* **40,** 1244–1249
12. Schreiber, G. (2002) *J. Endocrinol.* **175,** 61–73
13. Prapunpoj, P., Richardson, S. J., and Schreiber, G. (2002) *Am. J. Physiol.* **283,** R885-R896
14. Blake, C. C., Geisow, M. J., Oatley, S. J., Rérat, B., and Rérat, C. (1978) *J. Mol. Biol.* **121,** 339–356
15. Hamilton, J. A., Steinrauf, L. K., Braden, B. C., Liepnieks, J., Benson, M. D., Holmgren, G., Sandgren, O., and Steen, L. (1993) *J. Biol. Chem.* **268,** 2416–2424
16. Hörnberg, A., Eneqvist, T., Olofsson, A., Lundgren, E., and Sauer-Eriksson, A. E. (2000) *J. Mol. Biol.* **302,** 649–669
17. Wojtczak, A., Cody, V., Luft, J. R., and Pangborn, W. (1996) *Acta Crystallogr. Sect. D Biol. Crystallogr.* **52,** 758–765
18. Monaco, H. L., Rizzi, M., and Coda, A. (1995) *Science* **268,** 1039–1041
19. Naylor, H. M., and Newcomer, M. E. (1999) *Biochemistry* **38,** 2647–2653
20. Sunde, M., Richardson, S. J., Chang, L., Pettersson, T. M., Schreiber, G., and Blake, C. C. (1996) *Eur. J. Biochem.* **236,** 491–499
21. Wojtczak, A. (1997) *Acta Biochim. Pol.* **44,** 505–517
22. Saraiva, M. J. (1995) *Hum. Mutat.* **5,** 191–196
23. Benson, M. D., and Uemichi, T. (1996) *Amyloid: Int. J. Exp. Clin. Investig.* **3,** 44–56
24. Plante-Bordeneuve, V., and Said, G. (2000) *Curr. Opin. Neurol.* **13,** 569–573
25. Connors, L. H., Richardson, A. M., Théberge, R., and Costello, C. E. (2000) *Amyloid: Int. J. Exp. Clin. Investig.* **7,** 54–69
26. Eneqvist, T., and Sauer-Eriksson, A. E. (2001) *Amyloid: Int. J. Exp. Clin. Investig.* **8,** 149–168
27. Kelly, J. W. (1996) *Curr. Opin. Struct. Biol.* **6,** 11–17
28. Kelly, J. W. (1998) *Curr. Opin. Struct. Biol.* **8,** 101–106
29. Nielsen, H., Engelbrecht, J., Brunak, S., and von Heijne, G. (1997) *Protein Eng.* **10,** 1–6
30. Hanahan, D. (1983) *J. Mol. Biol.* **166,** 557–580
31. McPherson, A. (1982) *Preparation and Analysis of Protein Crystals*, John Wiley and Sons, New York
32. Sauer, U. H., and Ceska, T. A. (1997) *J. Appl. Crystallogr.* **30,** 71–72
33. Otwinowski, Z., and Minor, W. (1997) *Methods Enzymol.* **276,** 307–326
34. Collaborative Computational Project, N. (1994) *Acta Crystallogr. Section D Biol. Crystallogr.* **50,** 760–763
35. Brünger, A. T., Adams, P. D., Clore, G. M., DeLano, W. L., Gros, P., Grosse-Kunstleve, R. W., Jiang, J. S., Kuszewski, J., Nilges, M., Pannu, N. S., Read, R. J., Rice, L. M., Simonson, T., and Warren, G. L. (1998) *Acta Crystallogr. Sect. D Biol. Crystallogr.* **54,** 905–921
36. Brünger, A. T. (1992) *Nature* **355,** 472–474
37. Jones, T. A., Zou, J. Y., Cowan, S. W., and Kjeldgaard, M. (1991) *Acta Crystallogr. Sect. A* **47,** 110–119
38. Murshudov, G. N., Vagin, A. A., and Dodson, E. J. (1997) *Acta Crystallogr. Sect. D Biol. Crystallogr.* **53,** 240–255
39. Kleywegt, G. J., and Jones, T. A. (1998) *Acta Crystallogr. D Biol. Crystallogr.* **54,** 1119–1131
40. Laskowski, R. A., Moss, D. S., and Thornton, J. M. (1993) *J. Mol. Biol.* **231,** 1049–1067
41. Harris, M., and Jones, T. A. (2001) *Acta Crystallogr. Sect. D Biol. Crystallogr.* **57,** 1201–1203
42. Kraulis, P. J. (1991) *J. Appl. Crystallogr.* **24,** 946–950
43. Merritt, E. A., and Bacon, D. J. (1997) *Methods Enzymol.* **277,** 505–524
44. Folli, C., Pasquato, N., Ramazzina, I., Battistutta, R., Zanotti, G., and Berni, R. (2003) *FEBS Lett.* **555,** 279–284
45. Blake, C. C., and Oatley, S. J. (1977) *Nature* **268,** 115–120
46. Wojtczak, A., Neumann, P., and Cody, V. (2001) *Acta Crystallogr. Sect. D Biol. Crystallogr.* **57,** 957–967
47. Wojtczak, A., Cody, V., Luft, J. R., and Pangborn, W. (2001) *Acta Crystallogr. D Biol. Crystallogr.* **57,** 1061–1070
48. Ciszak, E., Cody, V., and Luft, J. R. (1992) *Proc. Natl. Acad. Sci. U. S. A.* **89,** 6644–6648
49. Wojtczak, A., Luft, J., and Cody, V. (1992) *J. Biol. Chem.* **267,** 353–357
50. Wojtczak, A., Luft, J. R., and Cody, V. (1993) *J. Biol. Chem.* **268,** 6202–6206
51. Peterson, S. A., Klabunde, T., Lashuel, H. A., Purkey, H., Sacchettini, J. C., and Kelly, J. W. (1998) *Proc. Natl. Acad. Sci. U. S. A.* **95,** 12956–12960
52. Klabunde, T., Petrassi, H. M., Oza, V. B., Raman, P., Kelly, J. W., and Sacchettini, J. C. (2000) *Nat. Struct. Biol.* **7,** 312–321
53. Ghosh, M., Meerts, I. A., Cook, A., Bergman, A., Brouwer, A., and Johnson, L. N. (2000) *Acta Crystallogr. Sect. D Biol. Crystallogr.* **56,** 1085–1095